

Thin Film Photonics

Oliver White

4 December 2020

Thin film stacks can be used to produce both anti-reflective coatings and mirrors that can reflect close to 100% of the incident light. In this project I used Python to develop a model to evaluate first single interfaces then a single film and finally to a multi-layer stack of films. The model returned the reflectivity of each scenario which in turn revealed that the greater number of alternating thin films of high and low refractive indices the greater the reflectivity. The results also suggest that the greater the difference in refractive index of the alternating films the greater the reflectivity. Both, the number of films and the refractive index difference are positively correlated with the range of wavelengths over which the reflectivity remained high.

Contents

1	Introduction	1
1.1	Context and Aims	1
1.2	Basic Theory	1
2	A Single Interface	3
2.1	The Fresnel Equations	3
2.2	The Initial Model	3
2.3	Initial Model Results & Discussion . .	4
3	Thin Film Interference	5
3.1	Adapting the Fresnel Equations	5
3.2	Progressing the Model	5
3.3	Thin Film Results and Discussion . . .	6
4	Multiple Films	7
4.1	Transfer Matrix Method	7
4.2	Increasing the Layers in the Stack . .	8
4.3	Varying Wavelength of the Incident Light	9
4.4	Varying the Refractive Index Difference	10
5	Summary	11
6	Future Work	12
A	Appendix	14

1 Introduction



Figure 1: Thin film photonics can be used to explain the colours seen on soap bubbles. [1]

1.1 Context and Aims

The physics of thin film photonics are used in a multitude of applications, from anti-reflective coatings on DVD's and CV's to optical filters and ultra-high reflectance mirrors [2]. Furthermore, commonly seen phenomena such as the bright colours seen with oil on water or on soap bubbles (as shown in Figure 1) can be explained through application of this region of physics.

In this project, I aimed to research how thin films can be used to increase the reflectivity of the incident light. I aimed to understand what factors could be changed to maximise the reflectivity, and to then discover how to increase the range of wavelengths whereupon the reflectivity is above a particular limit. A practical use of this type of mirror would be in creating a laser reflector as typical reflecting surfaces have a low resistance to the damage that can be caused by laser intensity [3].

In order to achieve this aim, I planned to calculate the reflectivity for a simple interface first, followed by a substrate with a thin film layer and finally a stack of multiple thin films. Due to the theoretical nature of the project, I used values for the parameters such as wavelength and refractive index that were within the physical norms. However, I decided to not use specific values as then the model could be used to study trends whilst being able to be easily adapted to compare any experimental data to the theoretical outcomes. I developed the models using the language Python [4] and the text editor Jupyter Notebooks[5]

and the code behind each stage is within the appendix.

1.2 Basic Theory

(a) TE polarisation

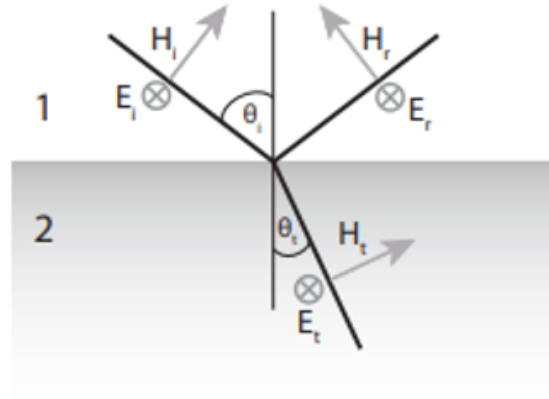


Figure 2: A schematic showing the reflection and transmission of Transverse Electric Light at a single interface between two media. Figure adapted from [6]

The behaviour of any electromagnetic wave is governed by Maxwell's equations and by applying boundary conditions one can understand how light acts at the interface between two media as depicted in Figure 2 and Figure 3. The specific equations in question are Faraday's law of induction (1) and Ampère's law (2) which are shown below.

$$\nabla \times \mathbf{E} = -\frac{\partial \mathbf{B}}{\partial t} \quad (1)$$

$$\nabla \times \mathbf{H} = \mathbf{J}_f + \frac{\partial \mathbf{D}}{\partial t} \quad (2)$$

For brevity, the full derivation of the boundary conditions is not included within this report however they appear when integrating each of these laws over an enclosed area that lies over the interface [7]. The relevant boundary conditions that are discovered are

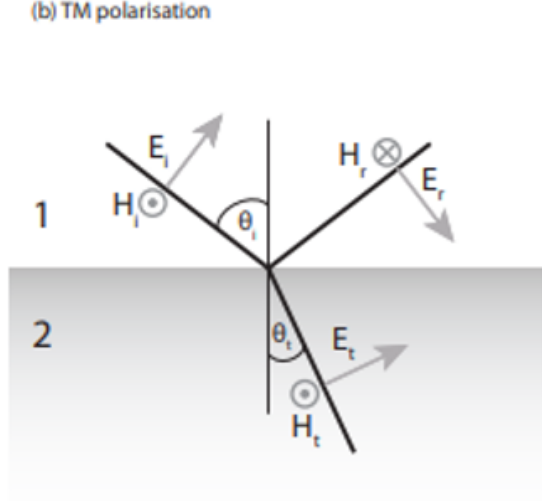


Figure 3: A schematic showing the reflection and transmission of Transverse Magnetic Light at a single interface between two media. Figure adapted from [6]

that both the tangential component of the Electric Field \mathbf{E} and Magnetic Field Strength \mathbf{H} are continuous at the interface in the absence of a surface current [8]. A plane wave solution to the Maxwell Equations is used throughout this report and is shown below [9].

$$\mathbf{E} = E_0 \exp(i[\mathbf{k} \cdot \mathbf{r} - \omega t]) \quad (3)$$

Here \mathbf{r} is the position vector, ω the angular frequency and t time. \mathbf{k} is defined as being the in-plane wave vector which is in the direction of propagation of the wave in the medium and of the magnitude $k = \frac{2\pi}{\lambda}$ where λ is the wavelength of the wave in the medium. As the wavelength is related to the refractive index n of the media we define the normal to the interface as the z direction so that the z -component of the wave-vector of the incident wave becomes:

$$k_{z,i} = \frac{2\pi}{\lambda} n_i \cos \theta_i. \quad (4)$$

Due to the tangential continuity of \mathbf{E} and \mathbf{H} and the dispersion relation [10] the angular frequencies of the incident, reflected and transmitted waves must

be equal. These conditions allow the derivation of Snell's law (shown below) and the law of reflection: $\theta_i = \theta_r$.

$$n_0 \sin \theta_0 = n_1 \sin \theta_1 = n_m \sin \theta_m = n_{m+1} \sin \theta_{m+1} \quad (5)$$

Maxwell's equations stipulate that \mathbf{k} , \mathbf{E} and \mathbf{H} must all be orthogonal which means that there are two obvious possibilities known as polarisations, for the direction of \mathbf{E} and \mathbf{H} . The two figures above show the two types of polarisation that will be considered within this report. Transverse-Electric (Figure 2) or s-polarisation (from the German senkrecht for perpendicular) is when the Electric field is perpendicular to the plane of incidence. The other is Transverse-Magnetic (Figure 3), or p-polarisation, where the Electric field is parallel to the plane of incidence.

The equations and definitions defined above are used throughout the report in the derivation of how the reflectivity and transmission of light at the interface of media changes with respect to different variables and in different cases.

2 A Single Interface

2.1 The Fresnel Equations

When considering the case shown in Figure 2 and Figure 3, by defining the complex amplitude reflection coefficient as,

$$r = \frac{E_r}{E_i} \quad (6)$$

and by using Maxwell's equations with the boundary conditions at an interface, as described in Section 1, one can derive the Fresnel Equations, as shown below. These describe the transmission and reflection amplitude coefficients for both TM and TE polarisation [11].

$$r_s = \frac{n_1 \cos \theta_i - n_2 \cos \theta_t}{n_1 \cos \theta_i + n_2 \cos \theta_t} \quad (7)$$

$$r_p = \frac{n_2 \cos \theta_i - n_1 \cos \theta_t}{n_2 \cos \theta_i + n_1 \cos \theta_t} \quad (8)$$

$$t_s = \frac{2n_1 \cos \theta_i}{n_1 \cos \theta_i + n_2 \cos \theta_t} \quad (9)$$

$$t_p = \frac{2n_1 \cos \theta_i}{n_2 \cos \theta_i + n_1 \cos \theta_t} \quad (10)$$

Here, n_i refers to the refractive index of media i ; θ_i denotes the incident and θ_t the transmitted angle as shown in Figure 2 and Figure 3. The incident and transmitted angle are related by Snell's Law(5).

Furthermore, the intensity reflection coefficient or simply the Reflectivity R , for both types of polarisation, can be defined as $R_{s,p} = |r_{s,p}|^2$ from the relationship between the intensity and amplitude of waves.

2.2 The Initial Model

To understand the characteristics of how light interacts at an interface between air and glass I decided to plot how $R_{s,p}$ changed as the incident angle changed. Here, my model assumed that the boundary between the media was perfectly flat and that the change in refractive index was immediate. Furthermore, I assumed that both media were perfectly transparent in order to ignore the absorption in each and focus solely on the reflection and transmission. This is a reasonable assumption to make for both air and glass as they both have negligible attenuation coefficients [12]. I also assumed that the wavelength and refractive index was constant throughout.

In this basic model I used refractive indices of 1 and 1.5 (to 2 significant figures) for air and glass respectively [13]. I then ran the model, with a greater difference in refractive index (by increasing the substrate index) to see if this had any effect on the reflectivity at normal incidence.

2.3 Initial Model Results & Discussion

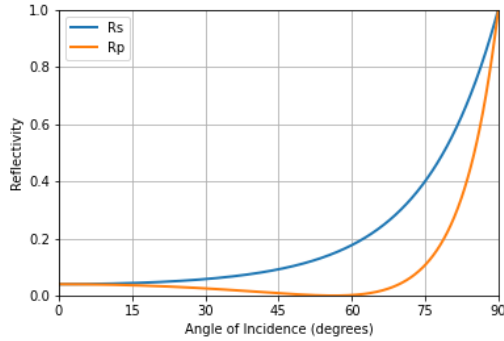


Figure 4: Variation in Reflectivity R as the angle of incidence θ_i changes between 0 and 90 degrees for light travelling between air and glass.

This graph shows several key features. One of which is that at normal incidence (i.e. $\theta_i = 0$) some of the light is still reflected. The specific value in my model is 0.04.

The angle at which the p-polarization drops to 0 is known as the Brewster angle. This can be easily seen by setting equation (8) equal to 0 which results in the Brewster angle equation:

$$\tan \theta_b = \frac{n_2}{n_1}. \quad (11)$$

For our model this returns a value of 56° .

Figure 4 is a well-documented representation of the Fresnel equations and thus had a very high reliability. The main source of error (aside from any error in the measurement techniques) had this been plotted using experimental data would likely have come from a variation in refractive index of the glass as different types of glass have some variation in their refractive index. Furthermore, the assumptions I made for this model would also have some effect on the reflectivity as some of the light would be partly absorbed and the surface wouldn't be perfectly flat.

Running the model with different values of the substrate index showed that increasing the substrate refractive index increased the value of reflectivity at

normal incidence. In general, the increase in index difference increased the reflectivity relative to the air-glass case. It also caused the Brewster angle to move closer to 90° as is expected from (11).

In the following stages of the project I used the key findings from this simple model to check that my models were returning reliable graphs.

3 Thin Film Interference

3.1 Adapting the Fresnel Equations

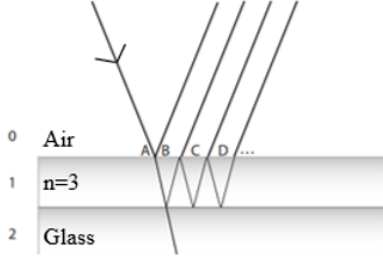


Figure 5: Light striking a thin film will infinitely reflect within the film and the reflected and transmitted waves can interfere causing increases in the reflection or transmission. Figure adapted from [14]

When considering the scenario depicted in Figure 5, the reflection amplitude coefficient for the entire slab r_{slab} can be derived using the Fresnel equations defined earlier and taking into account the phase shift that occurs at reflections each reflection [15]. The derivation considers a geometric sum of all of the reflections at points A, B, C, D.....etc. This derivation returns the following formula for the reflection of the slab:

$$R_{slab} = \left| \frac{r_{01} + r_{12} \exp(2ik_{z,1}d)}{1 + r_{01}r_{12} \exp(2ik_{z,1}d)} \right|^2 \quad (12)$$

Here, R_{ab} refers to the amplitude reflection coefficient defined earlier in (8) and (7). $k_{z,1}$ is the wave vector defined earlier in (4) and d is the thickness of the thin film.

3.2 Progressing the Model

I added a thin film of refractive index 3 and then varied the thickness of the thin film between 0-1000nm for light at normal incidence. I decided on a 3 for the refractive index as this was within the range of commonly accepted values of refractive index for common dielectric transparent media. I hypothesized that the reflectivity would oscillate, with peaks and troughs related to the refractive index.

To model this I simply plotted the equation for reflectance with a thin film against a range of thicknesses, setting the wavelength and angle of the incident light constant at 500nm and 0 degrees respectively. By using these conditions the real part of this exponential would reduce to $\cos(\frac{2\pi}{\lambda}nd)$. This would oscillate between -1 and 1 depending on the value of d .

I kept my initial assumptions of perfect flatness, transparency and a refractive index that was constant throughout.

3.3 Thin Film Results and Discussion

I saw from the results of this model (Figure 6) that the reflectivity did indeed oscillate and that the peaks were when $d = \frac{\lambda}{4n}$. Furthermore, the troughs of the reflectivity R occur at values equal to $d = \frac{\lambda}{2n}$. Both findings support the theory and my hypothesis, above. The peak reflectivity R returned for our parameters was 0.51 (to two significant figures). The increase in reflectivity at normal incidence in comparison to the single interface model supported my research that adding thin films would increase the reflectivity. A single thin film however was not enough to increase the reflectivity to close to 100%.

difficulties in creating films this thin. Thus for real experiments it could be advantageous to reduce the refractive index so as to increase the frequency of the oscillations in Figure 6 and thus potentially improve the accuracy. From Section 2, I knew that a reduction in the refractive index difference at normal incidence would reduce the peak reflectivity.

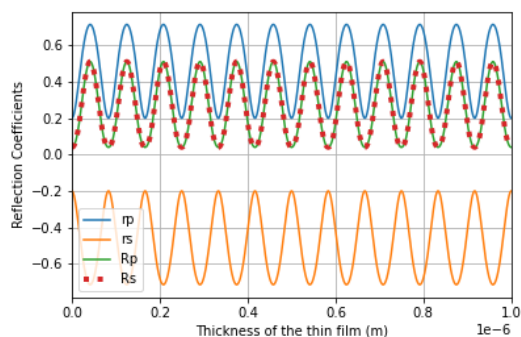


Figure 6: The Reflectivity oscillates, peaking when $d = \frac{\lambda}{4n}$ and dips when $d = \frac{\lambda}{2n}$

Some other important features I noted about this graph are as follows. The value of the reflection intensity R when the thickness of the film was 0 was 0.04 which was the same value as my single interface model. This was a positive sign that my model was returning reliable and accurate results. R_s and R_p were identical whilst r_s and r_p were the opposites of each other, which makes sense from the definitions of the two types of polarisations.

In order to return the maximum reflectivity a thin film of 41.6nm would have to be used or 83.3nm for the maximum transmission. Creating a thin film that was measurably better at either transmission or reflection would therefore need a very high level of accuracy. In reality there are likely to be practical dif-

4 Multiple Films

4.1 Transfer Matrix Method

The final step of the experiment was to further the model to include multiple layers of thin films of alternating high and low refractive index. This is known as a Bragg mirror and can be used to increase the reflectivity to close to 100% for a narrow range of wavelengths [16]. I wanted to research what the relationship was between the number of films in the stack and the reflectivity at normal incidence.

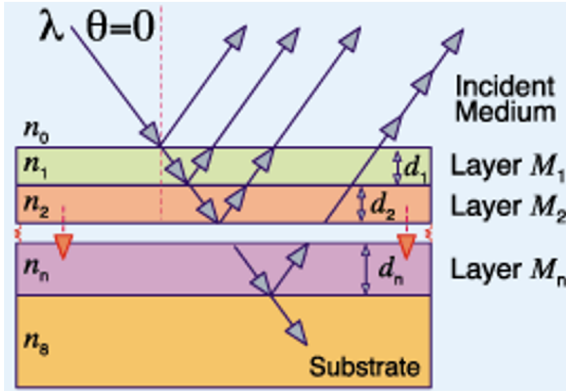


Figure 7: Incident light of wavelength λ strikes the multilayer stack and interacts with the multiple layers. Figure adapted from [17]

To do this I used one of the transfer matrix methods, specifically by Hayfield and White [18]. The method involves successive multiplication of matrices which represent the reflectivity between each respective layer. By applying Fermat's principle [19] there is also an additional matrix applied when travelling between layers to take account of the phase shift of travelling between media. For our model as shown in Figure 7, assuming n thin films layered between an infinite incident medium and upon another infinite substrate, the transfer matrix \mathbf{S} is given by:

$$\mathbf{S} = \frac{1}{t_{s,p}^{0,1}} \begin{bmatrix} 1 & r_{s,p}^{0,1} \\ r_{s,p}^{0,1} & 1 \end{bmatrix} \cdot \begin{bmatrix} e^{-i\gamma_1} & 0 \\ 0 & e^{i\gamma_1} \end{bmatrix} \cdot \frac{1}{t_{s,p}^{1,2}} \begin{bmatrix} 1 & r_{s,p}^{1,2} \\ r_{s,p}^{1,2} & 1 \end{bmatrix} \cdot \begin{bmatrix} e^{-i\gamma_2} & 0 \\ 0 & e^{i\gamma_2} \end{bmatrix} \cdots \begin{bmatrix} e^{-i\gamma_n} & 0 \\ 0 & e^{i\gamma_n} \end{bmatrix} \cdot \frac{1}{t_{s,p}^{n,sub}} \begin{bmatrix} 1 & r_{s,p}^{n,sub} \\ r_{s,p}^{n,sub} & 1 \end{bmatrix} \quad (13)$$

Where $t_{s,p}^{a,b}$ and $r_{s,p}^{a,b}$ are the Fresnel coefficients defined earlier in (7), (8), (9) and (10) and

$$\gamma_i = k_{z,i} d_i = \frac{2\pi}{\lambda} n_i \cos \theta_i d_i \quad (14)$$

using (4) and where d_i is the thickness of the i^{th} layer.

As a result of (13) the transfer matrix \mathbf{S} will always be of the form of a 2x2 matrix as shown below.

$$\mathbf{S} = \begin{bmatrix} S_{11} & S_{12} \\ S_{21} & S_{22} \end{bmatrix} \quad (15)$$

From this matrix the Fresnel coefficients can be calculated for the stack by:

$$\begin{aligned} r &= \frac{S_{21}}{S_{11}} \\ t &= \frac{1}{S_{11}} \end{aligned} \quad (16)$$

4.2 Increasing the Layers in the Stack

In order to progress the model I added multiple thin films to the single thin film of the previous model and kept the angle of incidence of the light at zero and the initial and substrate media as air and glass respectively. I chose alternating thin films each of which had a respective thickness $d_i = \frac{\lambda}{4n_i}$ which I knew from my earlier model in Section 3 would result in constructive interference and thus an increase in the reflection amplitude coefficient. I then plotted how $r_{s,p}$ and $R_{s,p}$ changed as I increased the number of pairs of films added to a single thin film model (that only contained the air, medium of index 3 and the glass). The pairs here refer to a high index layer and a low index layer. The model could run using any values of refractive index of the initial medium, substrate, or films, along with any value for the wavelength, however to remain consistent with my previous model I kept the wavelength along with the initial and substrate media constant and used a value of 3.0 for the high refractive index media and 2.0 for the low refractive index media. Thus, in the following results the total number of layers of films L is related to the number of pairs P by $L = 2P + 1$ due to the initial thin film.

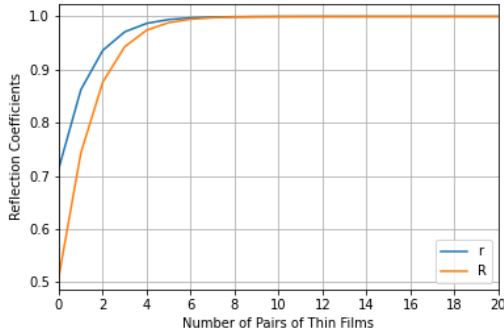


Figure 8: This graph demonstrates how increasing the number of pairs of alternating thin films of high and low refractive index causes the reflectivity to increase; tending towards 100% for high numbers of films

The results of this model as shown in Figure 8,

demonstrated that the greater the number of pairs (and thus layers) the greater the reflectivity. The reflectivity exponentially increased towards 100% as the number of layers increased. Closer analysis of the high reflectivity regions, as shown in Figure 9 show that for this particular set of values of wavelength, high, low and substrate refractive index, as few as 6 pairs (or 13 films in total) would give a reflectivity R of over 99%.

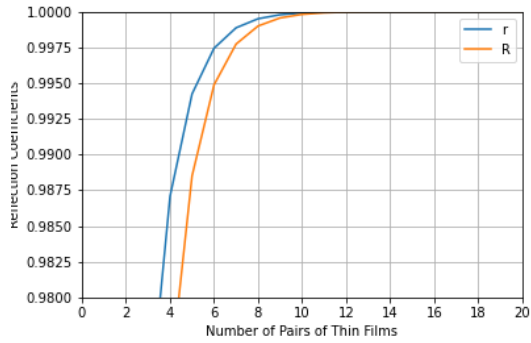


Figure 9: The reflectivity tends to 100% as the number of pairs increase.

4.3 Varying Wavelength of the Incident Light

Up until this point the model had only considered light of a specific wavelength. However, in reality a range of wavelengths could strike the multilayer stack. Therefore, I adapted the model to include a range of wavelength around the central wavelength (λ_0) that I had used to determine the thickness of each layer. I hypothesized that the graph produced would show peak reflectivity at the central wavelength and then decay exponentially on either side of this value [20]. Moreover, I hypothesized that a greater number of films would give rise to a wider range of wavelengths where the reflectivity was high.

When using this adaptation of the model, I kept my key assumptions the same as well as the same values of refractive index as in the previous stage. I varied the wavelength between 300nm and 700nm with a central wavelength of 500nm used and then calculated the reflectivity for this range of wavelengths to return Figure 10.

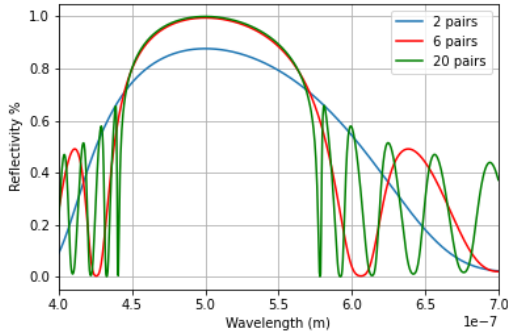


Figure 10: Reflectance variation with wavelength around a central wavelength of 500nm for thin film stacks with different numbers of pairs of thin films.

My hypothesis was partly correct as the reflectance does peak around the central wavelength however the behaviour on either side of this shows the reflectance oscillating with decreasing amplitude. For values of $\lambda > \lambda_0$ the frequency of the oscillations are increasing, and the amplitude is decreasing, with the frequency and the peak amplitude positively correlated to the number of pairs. When $\lambda < \lambda_0$ the peak amplitude of the oscillations also decreased, however the frequency remained constant and greater than the frequency the other side of λ_0 . Figure 10 shows only from 400-700nm as the results from 300-400nm contained very similar high frequency oscillations, similar to from 400-500nm, and these results made the graph more difficult to understand.

The results also showed that the more layers of thin films the greater the peak reflectivity, from 2 pairs where R was 88% (to 2 significant figures) to R being 100% (to 2 significant figures) for 20 pairs. This is in keeping with the trends and previous results which suggests a good level of reliability in this model.

My prediction that an increase in pairs would decrease the sharpness of the peak is correct with the range of high reflectivity wavelengths increasing as the number of pairs increase, anywhere in the top reflectivity ranges ($R > 0.8$). For lower reflectivity, the case becomes more complex as the higher the number of pairs the more sharply the reflectivity decreases around λ_0 .

Furthermore there is very little difference between the 6 pairs and 20 pairs lines in the high reflectivity regions ($R > 0.8$) which suggests that increasing the number of layers will not drastically improve the range of wavelengths over which the reflectivity is high.

In practise, the more layers added would increase the error in the reflectivity due to the error in the thickness of each layer contributing to the total error. This would suggest that creating a multi-layered stack with 6 films would give approximately the same range of wavelengths over which the reflectivity was high and reduce the potential error in creating very thin films.

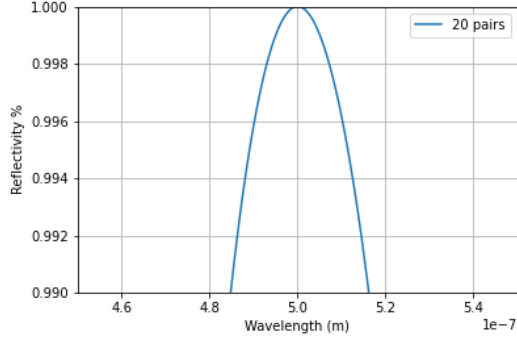


Figure 11: A section of Figure 10 showing the range of wavelengths (31nm) where the reflectivity of 20 pairs is greater than 99%.

4.4 Varying the Refractive Index Difference

This model also showed that a difference in refractive index between the alternating layers affected the shape of the graph, as shown in Figure 12.

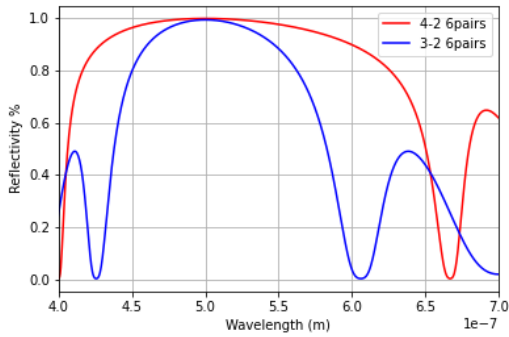


Figure 12: The difference in refractive index between the alternating layers affect the range of high reflectivity wavelengths. '4-2' denotes a high and low index of 4 and 2, while '3-2' has a high index of 3 and low index of 2.

This graph showed that changing the high refractive index (n_{high}) from 3 to 4 made the peak around the central wavelength much broader. This would allow a wider range of wavelengths that returned high

reflectivity.

I then decided to plot the relationship between the difference in refractive index and the range of wavelengths where the reflectivity was above a set limit. I decided to set my limit at $R > 0.99$, however the model could be run with any lower limit for the reflectivity. I then calculated the range of wavelengths over which 6 pairs had a value of $R > 99$ and plotted this range against values of refractive index difference. This model kept the low refractive index constant (at either 2 or 3) and then increased the higher index relative to the lower index. I hypothesised, based on the results in previous sections that the result would show a positive correlation between index difference and the range of high reflectivity wavelengths. I maintained the same assumptions as my previous model.

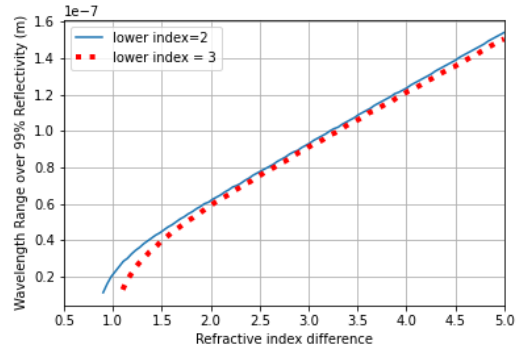


Figure 13: The range of high reflectivity wavelengths increases as the difference in refractive index increases.

The results here clearly support my hypothesis that increasing the difference in the refractive index did increase the range of high reflectivity wavelengths. Furthermore, the relationship is linear excluding when the difference is small. Therefore, I can conclude that in order to increase the range of high reflectivity wavelengths a multilayer stack that used alternating high and low refractive indices that had a large value of $n_{high} - n_{low}$ would be most effective.

The x-scale on this graph goes up to an index difference of 5 which would represent a value of n_{high} of

7 or 8. However, most common tables of refractive indices only contain materials with values in the range of 1-4.01 [21]. This would suggest that in practicality an absolute maximum index difference of 3 could be achieved. This would represent a range of 92nm over which the reflectivity was greater than 99% for 6 pairs.

The main errors with this initial conclusion are twofold. The first comes from the same assumption as in the previous section: that the refractive index of the media is constant with wavelength. In practise for many materials this is not the case [22] and dependant of the relationship between the media's index and wavelength it could affect the model drastically. The other error is that the greater the refractive index the more difficult it would become to create the thin film as the thickness would need to be smaller which could result in greater a greater error margin. Therefore, in practice, this increase in error could result in having to choose a smaller value for n_{high} and thus reducing the maximum feasible index difference.

lengths increasing linearly with index difference.

For example, 21 layers of alternating high and low index (3 and 2 respectively) could be used to increase the reflectivity to over 99.9% at for light at the central wavelength, and over 99% for a range of 31nm. Alternatively, 13 layers could have an 80nm (to 2 significant figures) range where the reflectivity was greater than 99%, if the difference in refractive index was 2.5 (to 2 significant figures).

These results could be used to create a ultra-high reflectivity mirror. The caveat to this, is that creating a thin film of only a few nano-meters thick could be very difficult to do accurately and thus careful consideration would be needed to decide how many layers of specific indices would be optimal for the required reflectivity level whilst maintaining the highest accuracy.

5 Summary

In this project I used the Fresnel equations, derived from Maxwell's equations to model the reflectivity of single interfaces, thin films and later multi-layer stacks of thin films. I decided throughout to keep the model as dynamic as possible so that it could plot the reflectivity for various refractive indices, wavelengths and thickness of films.

By building up the model through the steps outlined in the report, I firstly discovered that by setting the thickness of the films to a value equal to a quarter of the incident wavelength divided by the refractive index of the film it would result in constructive interference in the reflected waves which would lead to an increased reflectivity. Next, I found that by increasing the number of pairs of layers of alternating high and low refractive index, the reflectivity would exponentially increase to close to 100% reflectivity for the incident wavelength. To increase the range of wavelengths around the central wavelength over which the reflectivity was high, a higher difference between the refractive index was required, with the range of wave-

6 Future Work

I set out to complete this project with the flexibility of modelling the widest range of parameters possible and thus I specifically didn't choose any particular media for the thin films, or substrate or any particular wavelength of light. Clearly, in a 'real world' scenario the input values could be made to match a specific set of physically meaningful values.

Firstly, the limitations of the theoretical nature of this project mean that comparing the results I obtained with any of my own experimental data was impossible. Thus, an obvious further step would be to apply the theoretical results in practice. One potential experiment would be to use plasma enhanced chemical vapor deposition to deposit thin films of SiO_2 and Si_3N_4 [23] and look at how the reflection and transmission varied with different numbers of layers and over different ranges of wavelength. One of the potential benefits of this experiment in comparison with my project would be it would allow me to analyse in more depth the accuracy to which the thin films could be made. As a result of this I could use my findings to allow me to determine what materials would return the optimal refractive index difference to give the largest range of high-reflectance wavelengths with a reasonable accuracy and the practicality of forming the thin films of correct thickness. Currently, analysing the error in the thickness of the films is a hypothetical exercise using very rough estimates, so by doing the experiment the error analysis could be in more depth.

Secondly, the code would require very little adaptation to calculate the transmission of the light through the interfaces of each scenario. An interesting comparison to make would be how the reflectivity and transmission compare across different wavelengths, and using different refractive indices.

Thirdly, a further step to take would be to include the absorption of the media within the model by introducing complex refractive indices. The attenuation of the light as it passes through the medium would reduce the reflection and transmission coefficients. However, modelling how the reflection and transmission change as the attenuation coefficient within the refractive index changes would be an en-

gaging further step to take. I believe that my model, and the code behind it, is dynamic enough that introducing this would be very feasible.

Finally, contemporary research is largely focused on surface modes arising from different types of thin films such as metal, crystals and dyes. By introducing complex refractive indices and with more research into how surface modes arise, it was suggested that our model could be used to explore the behaviour of the surface modes. This future work would be dependent on completing my third recommendation for future work above, however this would be the direction in which to subsequently take the project.

References

- [1] <https://www.ecosia.org/images?q=soap> accessed 1st December 2020
- [2] H. A. Macleod. *Thin -Film Optical Filters*. Institute of Physics Publishing, 3 edition, 2001
- [3] https://www.rp-photonics.com/laser_mirrors.html accessed 24th November 2020
- [4] <https://www.python.org/>
- [5] <https://jupyter.org/>
- [6] Baptiste Auguié, *Fresnel formulæ*, 1st July 2009, pg1
- [7] John E. Davis *Multilayer Reflectivity* 5th January 2014, pg6
- [8] The Feynman Lectures on Physics Vol. I Ch. 33
- [9] Leandro N. Acquaroli, *Matrix method for thin film optics*, September 21, 2018
- [10] David Morin *Waves* Chapter 6
- [11] Baptiste Auguié, *Fresnel formulæ*, 1st July 2009, pg3
- [12] <https://www.sciencedirect.com/topics/physics-and-astronomy/attenuation-coefficients> accessed 25th October 2020
- [13] <https://www.britannica.com/science/refractive-index> accessed 25th October 2020
- [14] Baptiste Auguié, *Fresnel formulæ*, 1st July 2009, pg4
- [15] Baptiste Auguié, *Fresnel formulæ*, 1st July 2009
- [16] https://batop.de/information/r_Bragg.html , accessed 19th November 2020
- [17] <https://spie.org/news/detection-reflections?SS0=1> accessed 2nd December 2020
- [18] J. P. Landry *OI-RD Microscopy*, 9th February 2012, Appendix B
- [19] The Feynman Lectures on Physics Vol. I Ch. 26
- [20] C.A.F.Marques, A. Pospori and D. J. Webb *Time-dependent variation of POF Bragg grating reflectivity and wavelength submerged in different liquids*, 2017
- [21] <https://www.physlink.com/reference/indicesofrefraction.cfm> accessed 3rd December 2020
- [22] Tara Henriksen, Terry Ring, Derrick Call, Eric Eddings, Adel Sarojim *Determination of Soot Refractive Index as a Function of Height in an Inverse Diffusion Flame* , March 2007,
- [23] <https://spie.org/news/detection-reflections?SS0=1> accessed 3rd December 2020

A Appendix

Within this appendix I am going to include the key code used behind each of my models.

```
In [ ]: n1 = 1.0 #refractive index for air
n2 = 1.5 #refractive index for glass

def Rs(thI):
    thT = np.arcsin((n1*np.sin(thI))/n2)

    return (np.abs(
        (n1 * np.cos(thI) - n2 * np.cos(thT)) /
        (n1 * np.cos(thI) + n2 * np.cos(thT))
    ))**2

def Rp(thI):
    thT = np.arcsin((n1*np.sin(thI))/n2)

    return (np.abs(
        (n1 * np.cos(thT) - n2 * np.cos(thI)) /
        (n1 * np.cos(thT) + n2 * np.cos(thI))
    ))**2
```

Figure 14: This code describes reflectivity for a single interface as a function of the two refractive indices and the angles of incidence and transmission.

```
In [3]: def rp(thI, n1, n2):
    thT = np.arcsin((n1*np.sin(thI))/n2)

    return (n2 * np.cos(thI) - n1 * np.cos(thT)) / (n2 * np.cos(thI) + n1 * np.cos(thT))

def rs(thI, n1, n2):
    thT = np.arcsin((n1*np.sin(thI))/n2)

    return (n1*np.cos(thI) - n2*np.cos(thT)) / (n1*np.cos(thI) + n2*np.cos(thT))

In [4]: def rp_slab(thI, d):
    return (rp(thI, 1,3) + rp(thI, 3,1.5)*np.cos(2*3*d*k0*np.cos(thI))) /
    (1 + rp(thI, 1,3)*rp(thI, 3,1.5)*np.cos(2*3*d*k0*np.cos(thI)))

def rs_slab(thI, d):
    return (rs(thI, 1,3) + rs(thI, 3,1.5)*np.cos(2*3*d*k0*np.cos(thI))) /
    (1 + rs(thI, 1,3)*rs(thI, 3,1.5)*np.cos(2*3*d*k0*np.cos(thI)))
```

Figure 15: This code returns the reflectivity of light striking a thin film for a given angle of incidence and refractive indices of the film and substrate.

```
In [15]: def rp(n1, n2):
    return (n2 - n1) / (n2 + n1) #equations simplify to these at normal incidence

def rs(n1, n2):
    return (n1 - n2) / (n1 + n2)

def t(n1, n2): #t_p = t_s at normal incidence
    return (2*n1) / (n1+n2)

In [16]: def I(n_a, n_b):
    x = (1/t(n_a, n_b))
    y = np.array([[1, rp(n_a, n_b)], [rp(n_a, n_b), 1]])
    return np.multiply(x,y) #this is working and returning the correct array

In [17]: def r(m0,n_h,n_l,n_s,p): #should give the matrix from which we can find r and t
    L = np.array([[1,0], [0,1]]) #the phase factor matrix for when d= wvl/4n and wvl is constant
    l_start = I(m0, n_h) #going from air to the first layer
    I_HL = np.matmul(L, I(n_h,n_l)) #high to low
    I_LH = np.matmul(L, I(n_l,n_h)) #low to high
    I_finish = np.matmul(L, I(n_h, n_s)) #going from the last layer to the substrate

    Q = np.matmul(I_HL, I_LH)
    S = np.matmul(l_start,np.matmul(matrix_power(Q,p),I_finish))
    return (S[1][0]/ S[0][0]).real
```

Figure 16: Here, the code returns a value for r at normal incidence for an alternating multi-layer stack where the refractive indices of all the media and the number of alternating pairs are stated.

```
In [83]: def I(n_a, n_b):
    x = (1/t(n_a, n_b))
    y = np.array([[1, rp(n_a, n_b)], [rp(n_a, n_b), 1]])
    return np.multiply(x,y) #this is working and returning the correct array

In [84]: def gam(lam):
    return 2*pi*lam0/4*(1/lam)

gam(lam0) #gives pi/2 as required

Out[84]: 1.5707963267948966

In [85]: def r(m0,n_h,n_l,n_s,p,lam): #should give the matrix from which we can find r and t
    L = np.array([(np.cos(-gam(lam))-np.sin(gam(lam))*1j, 0),
    [0, np.cos(gam(lam))+np.sin(gam(lam))*1j]])
    l_start = I(m0, n_h) #going from air to the first layer
    I_HL = np.matmul(L, I(n_h,n_l)) #high to low
    I_LH = np.matmul(L, I(n_l,n_h)) #low to high
    I_finish = np.matmul(L, I(n_h, n_s)) #going from the last layer to the substrate

    Q = np.matmul(I_HL, I_LH)
    S = np.matmul(l_start,np.matmul(matrix_power(Q,p),I_finish))
    return (S[1][0]/ S[0][0]).real
```

Figure 17: This code builds on the previous model and returns r similarly, however the wavelength of the incident light is now included as a variable.

```

In [9]: def index_diff(n_h,n_l):
        return (n_h-n_l)

In [10]: def stop_band1(n_h, n_l,wvl1,wvl2):
        for i in np.linspace(wvl1,wvl2,1000): #800nm to 1200nm
            if R(1,n_h,n_l,1.5, 6,i) > 0.99:
                return i

In [12]: def stop_band2(n_h, n_l,wvl1,wvl2):
        for i in np.linspace(wvl2,wvl1,1000): #1200nm to 800nm
            if R(1,n_h,n_l,1.5, 6,i) > 0.99: #using the case with 20 pairs
                return i

In [14]: def stop_band_width(n_h,n_l,wvl1,wvl2):
        return stop_band2(n_h,n_l,wvl1,wvl2) - stop_band1(n_h,n_l,wvl1,wvl2)

In [29]: x2 = np.linspace(2.9,7,100) #high indexes array
        y2 = index_diff(x2,2) #array for our index differenece values

        p2 = x2.tolist() #high indexes list
        low2=[]
        for i in p2:
            low2.append(stop_band_width(i,2,0.0000003,0.0000007))

In [30]: x3 = np.linspace(4.1,8,100) #high indexes array
        y3 = index_diff(x3,3) #array for our index differenece values

        p3 = x3.tolist() #high indexes list
        low3=[]
        for i in p3:
            low3.append(stop_band_width(i,3,0.0000003,0.0000007))

```

Figure 18: This figure uses the previous code to return values for the range of wavelengths over which the reflectivity is greater than the set parameter. It also produces a simple function for the difference in refractive index.